



20 TeV p Accelerators and $\bar{p}p$ Collider

L.C. Teng

January 28, 1980

This is a summary of the work done at the Second ICFA Workshop on Accelerator and Detector Possibilities and Limitations held in Les Diablerets, Switzerland on October 4-10, 1979. Members of the group studying this subject are E.D. Courant, V.P. Dzhelepov, L. Ho, N.M. King, C. Pellegrini, I.A. Shukeilo, A.V. Tollestrup, V.A. Yarba and L.C. Teng (Convenor). Most of the details of the studies will appear as individual contributed papers in the Proceedings.

Common Lattice for p Accelerator and $\bar{p}p$ Collider

A. Lattice

We found no reason to deviate from the tried and true separated function FODO cells. For a given cell length the maximum amplitude function, β_{\max} , or maximum beam size has a shallow minimum at a phase advance of $\sim 76^\circ$. However, for beam manipulation it is desirable to have phase advances which are simple fractions of 360° . The usual practice is to adopt the somewhat higher than optimum phase advance per cell of 90° . Our discussions here are based mainly on the 90° -cell. On the other hand the 60° -cell also has several advantages. 60° is about as far from 76° as 90° and gives roughly the same β_{\max} , but requires weaker quadrupoles. Lattice using 60° FODO cells are discussed separately in a contributed paper.

General specifications of the lattice are the following:

1. As for the first Workshop we assumed a top energy of 20 TeV, a peak magnetic field of 10 T, a pulse period of 100 sec and a beam intensity of 10^{15} protons per pulse or, equivalently, 10^{13} p/sec.
2. For the ring magnets the aperture is likely determined by mechanical considerations for fabrication and is therefore independent of energy. Present experiences show that an aperture radius of 3-4 cm is about the smallest which can be fabricated conveniently. We took an aperture radius of 4 cm. For a quadrupole with pole tip field of 10 T this gives a field gradient of $B' = 250$ T/m.
3. As was already mentioned we used 90° separated-function FODO cells.
4. We assumed a minimum of 8 long straight sections. An example of the assignment of functions to the long straight sections is the following:

- 1 for injection in both directions.
- 1 for accelerating RF cavities.

The RF systems must have the capability of varying the relative phase of the counter-rotating beams so as to adjust the azimuthal location of the collision region.

- 1 for beam dump in both directions

In a superconducting magnet ring near perfect beam dumps are a necessity.

- 1 for extraction of the p beam to fixed targets
- 4 for colliding beams (ep, $\bar{p}p$, pp, etc.).

Depending on the demand for colliding beams 8 straight sections may not be enough. More straight sections can always be added with a corresponding increase in circumference. Most of these straight sections must be specially matched to give the desired beam characteristics such as high β , low β , zero dispersion (η), etc. But here, without having these special function matched insertions specified, we shall simply assume that all straight sections are bridged across by continuations of the FODO cells with the dipoles omitted. Multiples of four 90°-cells will give unit transfer matrix and hence give perfect matching for both β and η .

5. Several lattices with different cell lengths (focusing strengths) are worked out and given in Table 1. The shortest cell (strongest focusing) assumed has roughly the same length as those of CERN-SPS and Fermilab Energy Doubler, and the longest cell (weakest focusing) assumed has a length roughly scaled from the 1-TeV Energy Doubler according to the conventional $\sqrt{\text{momentum}}$ law. One intermediate case is also included. A FODO cell with 4 dipoles in a half-cell is shown in Figure 1.

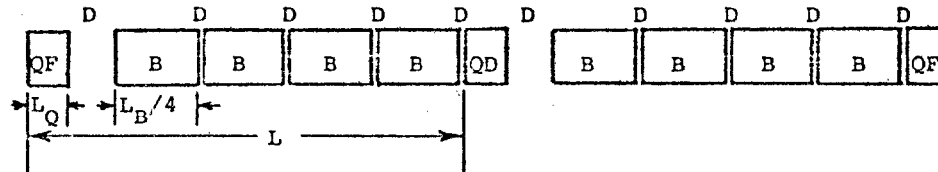


Figure 1 A FODO cell with 4 dipoles per $\frac{1}{2}$ -cell

B. Matched insertions

Experiences show that nearly all matched insertions can be made tunable over a sufficiently wide range by the addition of a few extra quadrupoles. Hence we do not see any problem of compatibility in the use of the ring as an accelerator and as a collider. The special function insertions can simply be tuned to yield the characteristics required for the application at the time.

The insertion which is related directly to the performance of the ring as a collider is the low- β insertion for the colliding straight section. The critical central part of the insertion is shown in Fig. 2.

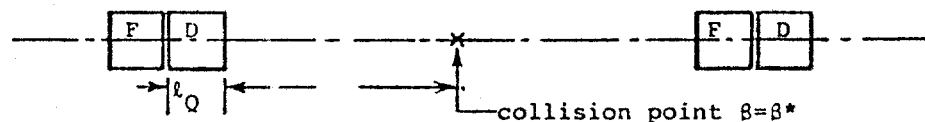


Figure 2 A low- β insertion

Table 1

Parameters of three lattices for the 20 TeV synchrotron

		<u>Strong</u>	<u>Medium</u>	<u>Weak</u>
Half cell length	L (m)	39	64	118
Dipole length/ $\frac{1}{4}$ cell	L_B (m)	4x6.25	8x6.25	16x6.25
Quad length/ $\frac{1}{4}$ cell	L_Q (m)	9.7	5.9	3.2
Drift length/ $\frac{1}{4}$ cell	L_D (m)	3.1+4x0.3	5.7+8x0.3	10.0+16x0.3
Total cell no.	N	936	484	242
Curved cell no.	N_B	840	420	210
Straight cell no.	N_S	8x12	8x8	8x4
Ring circumference	$2\pi R$ (km)	73.01	61.95	57.11
Ring radius	R (km)	11.62	9.86	9.09
Bending circumference	$2\pi\rho$ (km)	42.00	42.00	42.00
Bending radius	ρ (km)	6.685	6.685	6.685
Circumference factor	R/ ρ	1.74	1.48	1.36
Dipole peak field	B (T)	9.98	9.98	9.98
Dipole no.	M_B	6720	6720	6720
Quad peak gradient	B' (T/m)	249.4	249.8	249.8
Quadrupole no.	M_Q	1872	968	484
Betatron tune	Q	234	121	60
Max. amplitude fcn.	β_{\max} (m)	133.2	218.5	402.9
Min. amplitude fcn.	β_{\min} (m)	22.9	37.5	69.1
Bend angle/ $\frac{1}{4}$ cell	θ (mrad)	3.74	7.48	14.96
Transition- γ	γ_t	213.4	108.5	54.2
Max. dispersion fcn.	η_{\max} (m)	0.395	1.296	4.779
Min. dispersion fcn.	η_{\min} (m)	0.189	0.619	2.282

The lower limit of β^* is given by an upper limit on the β value at the first quadrupole doublet going away from the collision point. We consider 1500 m as a safe upper limit. Taking the drift distance from the collision point to the first doublet to be 50 m we get as a safe value

$$\beta^* \approx 2 \text{ m.}$$

The focal length of the doublet should be approximately half the distance from the collision point to the midpoint of the doublet. Using thin lens approximation this condition gives

$$\frac{1}{l_Q} \left(\frac{B\rho}{B'l_Q} \right)^2 = \frac{l+l_Q}{2}.$$

With $l = 50 \text{ m}$, $B\rho = 66.7 \text{ kTm}$ and $B' = 250 \text{ T/m}$; this gives $l_Q \approx 13 \text{ m}$, a reasonable value.

For smaller l , one can contemplate lower β^* . For example, with the same degree of conservatism one can obtain $\beta^* = 1 \text{ m}$ for $l = 35 \text{ m}$. For this study we adopted the higher value of $\beta^* = 2 \text{ m}$.

C. Error considerations

One of the criteria for choosing among the 3 cases of different focusing strengths is the consideration of their sensitivities to errors in construction. Generally, stronger focusing lattice is less sensitive to dipole errors but more sensitive to quadrupole errors and vice versa. The two most prominent linear error effects are the closed-orbit distortion caused by field errors $\frac{\delta B}{B}$ in the dipoles and misalignments δx of the quadrupoles; and the half-integer stop-band caused by non-zero field gradients $\frac{B'}{B}$ in the dipoles and gradient errors $\frac{\delta B'}{B'}$ in the quadrupoles. With the best estimates of these errors the effects are as follows:

Table 2

Effects of linear construction errors in the three lattices

	<u>Strong</u>	<u>Medium</u>	<u>Weak</u>
<u>Closed-orbit distortion (mm)</u>			
$\left(\frac{\delta B}{B} \right)_{\text{rms}} = 10^{-3}$	4.4	7.2	13.3
$(\delta x)_{\text{rms}} = \frac{1}{4} \text{ mm}$	23	16	12
<u>Half-integer stop-band width</u>			
$\left(\frac{B'}{B} \right)_{\text{rms}} = 5 \times 10^{-3} \text{ m}^{-1}$	0.0058	0.0096	0.0176
$\left(\frac{\delta B'}{B'} \right)_{\text{rms}} = 10^{-3}$	0.024	0.017	0.012

These values indicate a preference for the Weak case. More extensive

studies of error effects will be presented in a separate contributed paper.

Later we will see that for $\bar{p}p$ colliding beams in order to reduce the beam-beam effect to a minimum the \bar{p} and p beams should be kept separated by electrostatic dipoles except at the point of collision. Here again, it is easier to separate the orbits in the weaker focusing lattice.

D. Terrain following

For ring radius ~ 10 km or larger the effect of earth curvature on the orbit is sizeable. Furthermore, the topography and geological structure of the site may require the ring to deviate from the ideal geometrical shape. It is therefore important to examine how large a deviation can be tolerated.

If the curvature of the ring center-line deviates from the ideal curvature by $\delta\kappa$, the displacement y of the closed orbit from the ring center-line is given by

$$\frac{d^2y}{ds^2} + \frac{B'}{B\rho} y = \delta\kappa$$

where s is the distance along the ring center-line. The solution of this equation can be scaled from the normal dispersion function, η , which satisfies an equation of the same form with $\delta\kappa$ replaced by the curvature κ of the closed orbit. Hence the solution is

$$y = \eta \frac{\delta\kappa}{\kappa}.$$

If the maximum allowable y is 1 cm ($\frac{1}{4}$ of the aperture radius) the maximum tolerable $\delta\kappa$ for the 3 lattices considered above are given in the first row of Table 3.

Table 3

Consequences of terrain following for the three lattices

	<u>Strong</u>	<u>Medium</u>	<u>Weak</u>
$\delta\kappa$ (for $y_{\max} = 1$ cm)	$\frac{1}{264}$ km	$\frac{1}{866}$ km	$\frac{1}{3195}$ km
η_v	0.021 m	0.067 m	0.248 m
$\Delta\eta_h$	0.001 m	0.003 m	0.012 m

These values show that some pre-designed bending must be introduced if the ring is to follow any terrain with curvature much larger than the earth curvature.

Vertical bending can best be introduced by rolling the dipoles. To give an idea of the magnitude involved, if the dipoles are rolled by an angle of 0.1 radian, the vertical curvature obtained will be $\frac{1}{10}$ the horizontal curvature, or $\sim \frac{1}{67}$ km which is adequate for most reasonable construction sites while the reduction of the horizontal curvature is only $\sim 0.5\%$. The vertical dispersion η_v introduced by this vertical bending and

the change in the horizontal dispersion $\Delta\eta_h$ depend on the gentleness and smoothness of the terrain. Generally, the wave length of the terrain is much longer than the betatron wave length. In this case, the dispersions for the 3 lattices are those given in Table 3. Even for the weak focusing lattice the values are entirely tolerable.

One concludes that gentle variations in terrain can be followed by tailoring the roll and alignment of the dipoles without creating much undesirable orbital effect. The only concern is the greater difficulty involved in surveying a non-planar and non-periodic ring lattice.

E. Coherent instabilities

Various coherent instabilities in the 20 TeV accelerator/collider were investigated. The detailed results will be presented in a separate contributed paper. At the assumed beam parameters and for any of the 3 lattices considered, all coherent instabilities are either non-existent or can be controlled by paying special attention to the impedance of beam surrounding components or by the use of feedback dampers.

In summary, the lattice requirements of a p accelerator and a $\bar{p}p$ collider are found to be quite compatible. The traditional lattice composed of separated function 90° or 60° FODO cells with cell length scaled from the Fermilab Energy Doubler roughly as the square root of momentum was found to be quite serviceable and near optimal. The consideration of colliding beams application made it desirable to include at least 8 long straight sections. Many of these straight sections must be matched with continuously tunable insertions for variable amplitude and, perhaps, dispersion functions. Thus, we are faced at the outset with a single period lattice. However none of these requirements are impossible or even overly demanding.

p Sources and $\bar{p}p$ Colliding Beams

A. Limitations of beam cooling schemes

1. Electron cooling

The effectiveness of electron cooling reduces rather sharply at high energies. To see this we need only a rough scaling law for the cooling time. The cooling time is ultimately controlled by the regime in which the divergence angle of the proton (or antiproton) beam is smaller than that of the electron beam. In this regime the cooling time τ is given approximately by

$$\tau = \frac{1}{4\sqrt{2}\pi} \frac{\beta\gamma_e^2}{r_e r_p n j L} \left(\frac{T}{mc^2}\right)^{3/2}$$

where

r_e, r_p = classical radii of electron and proton

L = Coulomb logarithm ≈ 20

j = electron current density

η = cooling duty factor
 T = electron temperature
 e, mc^2 = charge and rest energy of electron.

Denoting the total electron current by I and the electron beam radius by σ we can write

$$j \propto \frac{I}{\sigma^2} \quad \text{and} \quad T \propto (\beta\gamma)^2 \sigma^2.$$

This gives

$$\tau \propto \frac{\beta^4 \gamma^5 \sigma^5}{\eta I}.$$

The electron beam radius must at least be equal to that of the proton beam. Assuming there is no other complication (unrealistic!) and we can indeed provide an electron beam as thin as the proton beam, we then have

$$\sigma \propto (\text{proton beam radius}) \propto (\beta\gamma)^{-1/2}$$

and

$$\tau \propto \frac{\beta^{\frac{3}{2}} \gamma^{\frac{5}{2}}}{\eta I}.$$

For an order of magnitude estimate we start from the present application of electron cooling to proton beams of $\sim 10^{-1}$ GeV with cooling times of $\sim 10^{-1}$ sec. If ηI were kept fixed which is difficult to do, the scaling in $\beta^{3/2} \gamma^{5/2}$ gives

$$\tau \sim 1 \text{ sec} \quad \text{at} \quad \sim 1 \text{ GeV},$$

$$\tau \sim 10^4 \text{ sec} \quad \text{at} \quad \sim 100 \text{ GeV},$$

$$\text{and} \quad \tau \sim 10^{10} \text{ sec} \quad \text{at} \quad \sim 20 \text{ TeV}.$$

Thus, we see that even with the overly optimistic assumptions of electron beam current and radius the cooling time is useful for accumulating \bar{p} only for energies $\gtrsim 1$ GeV. Cooling times of the order of an hour are useful for counteracting beam broadening caused by beam-beam effects, but are too long for application in the \bar{p} source.

2. Stochastic cooling

The cooling rate is limited by the available amplifier power. With present technology cooling times of the order of a few seconds can be contemplated only at proton (or antiproton) energies below ~ 10 GeV. Again, cooling times of the order of an hour can be obtained at energies up to a few hundred GeV and are useful for stabilizing the beams against beam-beam effects.

3. Synchrotron radiation cooling

The synchrotron radiation energy loss per turn, U , and damping

rate, $\frac{1}{\tau}$, for protons are given respectively by

$$U = \frac{4\pi}{3} \frac{r_p}{\rho} \gamma^4 (mc^2)$$

$$\frac{1}{\tau} = \frac{c}{2\pi R} \frac{U}{2E} = \frac{c}{3} \frac{r_p}{\rho R} \gamma^3.$$

With

$$\begin{aligned} mc^2 &= 938 \text{ MeV} = \text{rest energy of } p \\ r_p &= 1.53 \times 10^{-18} \text{ m} = \text{classical radius of } p \\ \gamma &= 2.13 \times 10^4 \text{ (at } E = 20 \text{ TeV)} \\ \rho &= 6.67 \times 10^3 \text{ m (at } B = 10 \text{ T)} \\ R &= 10^4 \text{ m (average of 3 lattices)} \end{aligned}$$

we get

$$\begin{aligned} U &= 0.19 \text{ MeV} \\ \tau &= 12.5 \text{ hr.} \end{aligned}$$

The damping rates in individual dimensions depend on the partition functions but are all of this order. These damping rates are close to being useful for counteracting the antidamping due to beam-beam effects, but are much too low for use in accumulating \bar{p} . In fact, with 20 TeV protons on target the energy of \bar{p} at peak production is only ~0.1 TeV. To scale down to this energy we make the most advantageous assumption that the magnetic guide field is kept fixed at 10 T. This gives $\rho \propto \gamma$, $R \propto \gamma$, and hence $\frac{1}{\tau} \propto \gamma$. At the production energy of 0.1 TeV the cooling time of \bar{p} is then ~2500 hours, entirely too long for whatever application.

The conclusion is that if cooling is used for accumulating \bar{p} it must be applied at energies well below ~10 GeV, preferably below ~5 GeV. Examples of \bar{p} sources employing beam cooling at low energies are described in a contributed paper. On the other hand if one accumulates \bar{p} at, say, 100 GeV, compared to accumulating at 5 GeV one gets an immediate advantage in production solid-angle of a factor $(20)^2$. Such a factor is difficult to regain by any of the cooling schemes. Thus, one may just as well collect the \bar{p} produced at high energy directly without cooling.

B. High energy accumulation of \bar{p}

The \bar{p} inclusive production cross-section is given by

$$\sigma_{\text{prod}} = \sigma' (mc^2)^2 \frac{\epsilon^2}{\pi a^2} \frac{\Delta p}{p}$$

where

$$\begin{aligned} mc^2 &= \text{rest energy of } \bar{p} \\ \epsilon &= \text{normalized transverse acceptance for } \bar{p} \\ a &= \text{radius of target (p beam spot)} \\ \frac{\Delta p}{p} &= \text{momentum acceptance for } \bar{p} \end{aligned}$$

and where the invariant cross-section σ' has the asymptotic value of $\sim 3 \text{ mb/GeV}^2$ for incident p energies above 1 TeV and for \bar{p} produced at rest in the center-of-mass frame of the incident p -nucleon system. The \bar{p} energy is therefore

$$E_{\bar{p}} = (mc^2 E_p/2)^{1/2}$$

where E_p is the energy of the incident proton. For $E_p = 20 \text{ TeV}$ we get $E_{\bar{p}} \approx 100 \text{ GeV}$. The optimum number of \bar{p} per incident p is, then

$$\frac{N_{\bar{p}}}{N_p} = \frac{\sigma_{\text{prod}}}{\sigma_{\text{abs}}} \times (\text{targeting eff.}).$$

With

$$\epsilon = 2 \times 10^{-4} \text{ m} \quad \left(\begin{array}{l} \text{source radius} = 0.15 \text{ mm} \\ \text{semi-cone angle} = 4 \text{ mrad} \\ \text{at } 100 \text{ GeV} \end{array} \right)$$

$$\frac{\Delta p}{p} = 2\%$$

$$a = 0.15 \text{ mm}$$

$$\sigma_{\text{abs.}} = \text{absorption cross-section of } \bar{p} \text{ in target} \approx 40 \text{ mb}$$

$$\text{targeting eff.} = 1/2$$

we get

$$\frac{N_{\bar{p}}}{N_p} \approx 4 \times 10^{-4}.$$

At 10^{13} p/sec we get $4 \times 10^9 \bar{p}/\text{sec}$ or $4 \times 10^{11} \bar{p}/\text{pulse}$ at 10^{15} p/pulse .

C. Stacking scenario and $\bar{p}p$ colliding beams.

We present here only one possible scenario. Others are given in contributed papers. In this scenario (see Fig. 3) we assume that there is

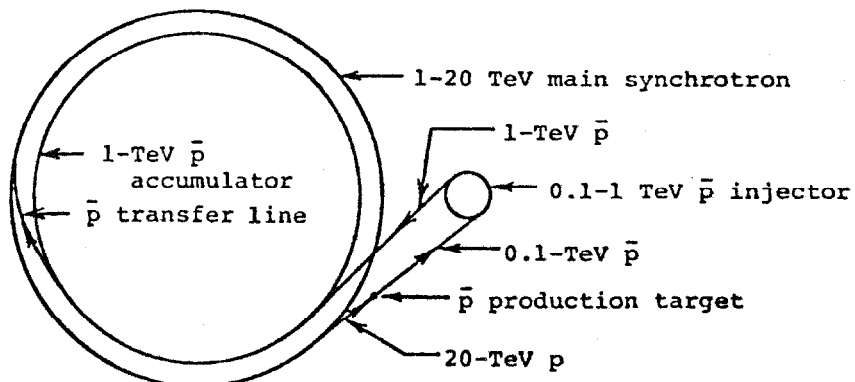


Figure 3. Production and accumulation of \bar{p}

a 1 TeV d.c. accumulator ring with the same circumference hence $\frac{1}{20}$ the total dipole strength as the 20 TeV main synchrotron and installed in the same tunnel. In addition, there is a 100 GeV to 1 TeV synchrotron with $\frac{1}{10}$ the circumference serving as injector. The 10^{15} p's at 20 TeV in the main synchrotron is first compressed by rf manipulations to $\frac{1}{10}$ the circumference, then extracted to hit the \bar{p} production target. The 4×10^{11} \bar{p} 's produced at 100 GeV is injected into the injector, accelerated to 1 TeV by an rf system with harmonic number 100, then injected into the d.c. accumulator ring. Ten main synchrotron pulses injected head-to-tail in the box-car fashion will fill the accumulator. The 4×10^{12} \bar{p} beam is then transferred to the main synchrotron and together with a 1-TeV, 10^{15} p beam injected in the opposite direction accelerated to 20 TeV each in 1000 bunches. The beams are then made to collide at a location with low- β^* . The luminosity is given by

$$L = \frac{\gamma f}{n} \frac{N_p N_{\bar{p}}}{\beta^* \epsilon}$$

With

$$\begin{aligned}\gamma &\approx 2 \times 10^4 \text{ (20 TeV)} \\ f &\approx \text{revolution frequency} \approx 5 \times 10^3 \text{ Hz} \\ n &\approx \text{number of bunches} = 10^3 \\ N_p &= 10^{15} \\ N_{\bar{p}} &= 4 \times 10^{12} \\ \beta^* &= 2 \text{ m} \\ \epsilon &= 2 \times 10^{-4} \text{ m}\end{aligned}$$

we get

$$L \approx 10^{32} \text{ cm}^{-2} \text{ sec}^{-1}$$

we assume here that the emittance of the p beam is deliberately blown up to equal that of the \bar{p} beam, namely 2×10^{-4} m. This is to reduce the beam-beam tune-shift of the \bar{p} to the value

$$\Delta Q_{\bar{p}} = \frac{r_p N_p}{n \epsilon} = 0.0077$$

which is slightly larger than the traditionally adopted upper limit of 0.005. Moreover, despite of the observation that tune-shifts from different collision points do not seem to add coherently, when the number of collision points around the ring is as high as 2000 it becomes necessary to keep the beams separated to avoid all collisions except the one used for physics experiment. The easiest way to do this is to introduce an n^{th} harmonic transverse electrostatic field where n is the integer nearest the betatron tune Q . This field will produce n^{th} harmonic distortion in the p and \bar{p} orbits opposite in phase. Take, as example, the weak focusing lattice with $R = 9.09$ km and $Q = 60.25$. To separate the orbits by ± 1 cm at the peak excursions we need 120 electrostatic dipoles each 2 m long, producing

a field of ~ 70 kV/cm, and arranged to give a 60th harmonic.

If the tune shift of 0.0077 at the only remaining collision point still proves to be excessive one must reduce N_p . In order not to lose luminosity the reduction in N_p should be compensated by an increase in $N_{\bar{p}}$ through e.g. momentum stacking in the accumulator ring. Without stacking the momentum spread in the \bar{p} beam is only $\pm 10^{-3}$ at 1 TeV and $\pm 0.5 \times 10^{-4}$ at the full energy of 20 TeV. In any case, useful luminosity can be obtained by accumulating \bar{p} 's produced only in a few tens of pulses or less than an hour.

The reason for having 1000 bunches in each beam is that now the luminosity of each collision between two bunches is only $2 \times 10^{25} \text{ cm}^{-2}$ and the probability of having two unresolvable events occurring in one collision is essentially zero. We should also point out that when the \bar{p} production target is struck by 10^{15} , 20-TeV protons in 20 μsec on a spot with radius 0.15 mm, it will surely explode. Thus, some mechanism must be designed to replace a new target for each incident pulse of protons. Even at the much lower level of proton beam power available today the \bar{p} production target is already approaching explosion and the target replacing mechanism may already be needed. Thus, such mechanisms are expected to be well developed by the time the 20-TeV synchrotron is in construction.

Discussions of Allowable Tune-Shifts

A meeting was held amongst all participants concerned with colliding beams to assess the present state of understanding of beam-beam effects and to discuss what limiting tune-shift values we should adopt at the Workshop for various colliding beam systems. The experimental and analytical informations available are summarized in the following.

A. Most of the electron or positron colliding beam systems are head-on collisions of bunched beams. Experiments on these machines give a maximum obtainable tune-shift, ΔQ_{max} , which increases with energy, E , but saturates at a value of ~ 0.05 . Below saturation the energy dependence can be fitted by

$$\Delta Q_{\text{max}} = a + bE \quad \text{or} \quad (a + bE^3)^{1/4}$$

In this region the tune-shift is presumably limited by the competition between the damping due to synchrotron radiation and the antidamping due to Arnold's diffusion. Depending on the detailed interpretation one can justify either the fits given above. At ~ 0.05 presumably the stochasticity limit (overlapping of stochastic layers of neighboring resonances) is reached and the tune-shift can go no higher under whatever condition.

When there are several collision points around the ring ΔQ_{max} should be interpreted as the quadrature sum of the tune-shifts from different collision points. This seems to be borne out by experiments.

B. For proton beams the only source of experimental information is the CERN-ISR which is a system of finite-angle crossings of continuous beams.

At low tune-shifts the beam life-time seems to decrease exponentially with increasing tune-shift; but there does not seem to exist any sharp limits. At tune-shifts larger than ~ 0.02 the beam life-time shortens to less than an hour and the colliding beams become difficult to use for physics experiments. No reliable observation has been made at tune-shifts close to 0.05. It is possible that as for electron beams a hard saturation limit of ~ 0.05 exists also for proton beams.

With negligible synchrotron radiation damping the life-time of a proton (or antiproton) beam is determined only by the Arnol'd diffusion. The theory of Arnol'd diffusion is not well enough developed to give a definitive formula for the life-time, but an exponential dependence on tune-shift is certainly not inconceivable.

During the Workshop an experiment was performed on the ISR to compare the life-times of bunched and continuous beams. No conclusive difference was observed. However, the tune shifts used for the experiment were low and the bunched beam had rather long bunches so that it could still be well approximated as a continuous beam.

C. For continuous beams crossing at a finite angle the beam-beam force is one-dimensional, acting only in the direction perpendicular to the beam crossing plane. This system should be the most stable and able to sustain the highest tune-shift. Long-bunched beams for which the bunch length is much larger than the width can be approximated as continuous beams as far as the dimensionality of the beam-beam force is concerned. But the particles execute synchrotron oscillations inside the bunch, and the particle density varies along the length of the bunch giving a small longitudinal field. Indeed numerical studies made on computers showed that bunched beams, even with long bunches, tend to be more unstable than continuous beams.

Head-on collisions give beam-beam forces which are two-dimensional acting in both the transverse dimensions. This system should be less stable than the case of finite-angle crossing. If, moreover, the beams are bunched into long bunches one would expect them to be further slightly less stable. The proposed $\bar{p}p$ colliding beams are head-on collisions of bunched beams and should therefore be less stable than the pp colliding beams in the ISR.

Of course, the worse case is the collision of short bunched beams for which the bunch length is comparable to the width. For either head-on collision or finite-angle crossing the beam-beam force is three-dimensional and the beams are expected to be least stable and able to tolerate the lowest tune-shift of all cases.

Although these qualitative comparisons of different cases are generally agreed to be valid, no one was able to make any quantitative or even semi-quantitative statement about these comparisons. Indeed no one is even sure whether the traditionally adopted tune-shift limit of 0.005 for the case of finite-angle crossing of continuous proton beams is optimistic or pessimistic. After lengthy discussions the attendees of the meeting decided to acknowledge the fact that no new information or understanding has been acquired since

the last Workshop by leaving the allowable values of tune-shift unchanged from those adopted before, namely

0.05 for e^+ and e^- beams

0.005 for \bar{p} and p beams

whether bunched or continuous and whether the collision is head-on or finite-angle.

D. The crucial question at this time is the beam-beam effect for $\bar{p}p$ colliding, i.e. the system of two-dimensional forces on bunched beams. It is next to impossible in the ISR to obtain head-on collisions or short bunched beams. Therefore it is unlikely that any information on the effects of higher-than-one dimensional forces can be derived from the ISR. Experiments are being prepared to study the stability of the SPS beam under the influence of a non-linear lens. This will give the effect of the two-dimensional non-linear forces of the lens on bunched beams. Of course the SPS beam bunches are not really short and the non-linear forces of the lens are quite different from the beam-beam forces. Nevertheless this could provide an experimental check against results obtained from computer simulation and give us much more confidence on the computer results for realistic systems.

High Field Superconducting Magnets and Radiation Shielding

Since it was anticipated that the next ICFA Workshop will be devoted exclusively to the study of high field superconducting magnets this subject was covered only casually and fragmentarily. Some of the topics investigated are described below.

A. We consider 10 T a realistic goal for magnets with some type of high field conductor. But the totality of efforts now devoted to the development of these conductors and magnets is very small. Listed below are all the real and virtual efforts we learned from inquiries made to the participants of the Workshop.

<u>Laboratory</u>	<u>Person in Charge</u>	<u>Field</u>	<u>Conductor</u>
LBL	Gilbert	7-10 T	Nb ₃ Sn, A-15 Compounds
BNL	Sampson	----	Nb ₃ Sn
RHEL	Martin	----	-----
Saclay	Desportes	>6 T	NbTi
Hitachi	-----	----	NbZrTi(50:40:10)
Karlsruhe	-----	----	-----

From the experiences gained in developing 5-T, NbTi magnets we can expect that a great deal of dedicated and concerted effort and time is needed if we want to have 10 T available at the time when physics requirement starts to demand 20 TeV.

B. The radiation heating and quenching of superconducting magnet by stray beam remains a serious problem in the application of superconducting magnets to accelerators and storage rings. The results of a detailed study of this effect is given in a contributed paper.

C. People have so far been reluctant to use superconducting magnet for field intensities less than 0.5 T because of the remanent field due to persistent currents in the conductors. But the accumulating experience at Fermilab is beginning to indicate that although the remanent field is sizeable it is repeatable from pulse to pulse and hence can be compensated by d.c. correction magnets. If this is true the broadened useful range of field will make superconducting machines much more versatile. The Fermilab experience and the evidence will be discussed in a contributed paper.

D. Radiation shielding at 20 TeV has some unique problems. These are discussed in a separate contributed paper.